DEVELOPMENT OF HYPERSPECTRAL IMAGING TECHNIQUE FOR THE DETECTION OF CHILLING INJURY IN CUCUMBERS; SPECTRAL AND IMAGE ANALYSIS

Y. Liu, Y. R. Chen, C. Y. Wang, D. E. Chan, M. S. Kim

ABSTRACT. *Hyperspectral images of cucumbers were acquired before and during cold storage treatment as well as during subsequent room temperature (RT) storage to explore the potential for the detection of chilling induced damage in whole cucumbers. Region of interest (ROI) spectral features of chilling injured areas, resulting from cold storage treatments at 0℃ or 5℃, showed a reduction in reflectance intensity during multi-day post-chilling periods of RT storage. Large spectral differences between good-smooth skins and chilling injured skins occurred in the 700- to 850-nm visible/NIR region. A number of data processing methods, including simple spectral band algorithms and principal component analysis (PCA), were attempted to discriminate the ROI spectra of good cucumber skins from those of chilling injured skins. Results revealed that using either a dual-band ratio algorithm ($Q_{811/756}$) or a PCA model from a narrow spectral region of 733- to 848-nm could detect chilling injured skins with a success rate of over 90%. Furthermore, the dual-band algorithm was applied to the analysis of images of cucumbers at different conditions, and the resultant images showed more correct identification of chilling injured spots than PCA method. The results also suggested that chilling injury was relatively difficult to detect at the stage of the first 0 to 2 days of post-chilling RT storage, due to insignificant manifestation of chilling induced symptoms.*

Keywords. *Hyperspectral imaging spectroscopy, Visible/near infrared spectroscopy, Algorithm, Principal component analysis, Chilling injury in cucumber.*

It is well known that many fruits and vegetables are sensitive to chilling and are damaged during the storage and transportation process at low temperatures. Cucumber is one of such produce and is apt to suffer chilling injury from relatively short periods of time at low temperatures. The major symptom of chilling injury in cucumber is surface pitting, which is then followed by water soaking associated with tissues collapse and shriveling. Extensive decay occurs when chilling injured cucumbers are returned to warmer temperatures, and damaged areas can become sites for further fungal decay and bacterial infection. Accumulated bacterial pathogens from these areas can be transmitted to humans by consumption of uncooked or mishandled cucumbers.

Article was submitted for review in September 2004; approved for publication by the Food & Process Engineering Institute Division of ASABE in August 2005.

Mention of a product or specific equipment does not constitute a guarantee or warranty by the U.S. Department of Agriculture and does not imply its approval to the exclusion of other products that may also be suitable.

The authors are **Yongliang Liu,** Visiting Chemist, Instrumentation and Sensing Laboratory, **Yud-Ren Chen, ASABE Member Engineer,** Research Leader, Instrumentation and Sensing Laboratory, **Chien Yi Wang,** Research Horticulturist, Produce Quality and Safety Laboratory, **Diane E. Chan,** Agricultural Engineer, Instrumentation and Sensing Laboratory, and **Moon S. Kim,** Research Physicist, Instrumentation and Sensing Laboratory, Henry A. Wallace Beltsville Agricultural Research Center, ARS, USDA, Beltsville, Maryland. **Corresponding author:** Yud-Ren R. Chen, Instrumentation and Sensing Laboratory, Henry A. Wallace Beltsville Agricultural Research Center, ARS, USDA, Building 303, BARC-East, 10300 Baltimore Ave., Beltsville, MD 20705; phone: 301-504-8450; fax: 301-504-9466; e-mail: cheny@ba.ars.usda.gov.

Chilling injury is of great concern to the fruit and vegetable industry because it can not only affect the safety/quality grade of the produce, but also cause significant economic losses. Hence, a variety of methods have been used to reduce the occurrence of chilling injury for cold-sensitive fruits and vegetables. These techniques include low temperature preconditioning, intermittent warming, waxing, genetic modification, and chemical treatments (Wang, 1993). Nevertheless, the development of rapid, non-destructive, and accurate techniques that are suitable for on-line and at-line operations is critical to increase the efficiency of cucumber safety/quality evaluation. Hyperspectral imaging spectroscopy can be the basis for the development of such techniques due to its non-invasive nature and capacity for large spatial sampling areas.

Hyperspectral imaging spectroscopy, which combines the features of imaging techniques and vibrational spectroscopy in the visible, near-infrared (NIR) and mid-infrared (IR) regions, has been developed as an inspection tool for quality and safety assessment of a number of agricultural and food products. Successful applications include the classification of chicken carcasses into wholesome and unwholesome classes (Lu and Chen, 1998), the detection of bruises and defects on apples (Lu, 2003; Lu et al., 1999; Mehl et al., 2002), and the determination of fecal contamination on apples and chicken carcasses (Kim et al., 2002; Lawrence et al., 2001; Mehl et al., 2004). However, hyperspectral-imaging technology currently cannot be directly implemented in automated on-line systems because current image acquisition and data analysis speeds are too slow for on-line operations.

To design rapid sensing instruments, namely multispectral imaging systems, several essential spectral bands (usually

  ISSN 0883−8542

two or three) are first sought through a variety of strategies, such as through the analysis of spectral differences in conventional visible/NIR spectra (Liu et al., 2003), the use of principal component loadings of principal component analysis (PCA) with conventional visible/NIR spectra (Windham et al., 2003), the visual observation of separation/contrast on images given different pre-processing treatments (Mehl et al., 2004), and the use of PCA on hyperspectral imaging data (Kim et al., 2002; Mehl et al., 2004). The selected wavebands should not only reflect the chemical/physical information in samples, but also maintain successive discrimination and classification efficiency.

The objectives of this study were: (1) to obtain the characteristic bands for chilling damaged cucumbers from region of interest (ROI) spectra in the 450- to 950-nm region, (2) to develop simple spectral waveband algorithms for the detection of chilling injury in cucumber from ROI data, (3) to validate the classification results using PCA, and (4) to apply the optimum algorithm for the analysis of hyperspectral images of cucumbers. The ultimate purpose was to lead to the development of faster and more efficient multispectral technique for real-time inspection of chilling injuries and defects for cucumber safety and quality.

Materials and Methods

Cucumbers and Chilling/Post-Chilling Treatments

Ninety-eight commercial-ready cucumbers were freshly picked from a farm in Beltsville, Maryland, during the 2002 harvest season. Only cucumbers that were free of damages, according to visual inspection, were used for the study. Ninety cucumbers were randomly subdivided into 30 groups of three cucumbers each, and each group was placed in a plastic bag punched with small holes to allow for air circulation. Fifteen groups were designated for cold storage at 0°C and the other 15 at 5°C, over a period of 15 days in two temperature-controlled and darkened storage rooms. Prior to the cold storage treatments, hyperspectral images were collected for all cucumbers. On each of the 15 days, one group was taken from each of the two cold storage rooms and moved to an air-conditioned laboratory maintained at a room temperature (RT) of 18°C to 20°C, where hyperspectral images were collected for the newly moved cucumbers. After scanning the images, the cucumbers were subsequently stored in this room for the remaining duration of the experiment. Also, on each day, hyperspectral images for all cucumbers previously moved to the RT laboratory were collected. The last two groups were moved to RT after 15 days of cold storage, and RT image collection for the cucumbers continued for 6 days afterwards. In addition, hyperspectral images were collected each day for eight cucumbers, in four groups of two cucumbers each, that were stored at RT in the laboratory for the entire duration of the experiment as control samples.

Hyperspectral Imaging Acquisition and ROI Spectra

A hyperspectral imaging system developed by the USDA Instrumentation and Sensing Laboratory was used to scan the cucumbers (Kim et al., 2001). It used a charge coupled device (CCD) camera system Spectra Video™ Camera (PixelVision, Inc., Tigard, Ore.) equipped with an imaging spectrograph SPECIM ImSpector version 1.7 (Spectral Imaging Ltd., Oulu, Finland). It was operated in a line-by-line scan mode, resulting in an image cube of 460 × 300 spatial and 112 spectral bands for each group of cucumbers. The spectral wavelength range was 447 to 951 nm with a 4.5-nm interval. Two 21-V, 150-W halogen lamps (Dolan-Jenner Industrious Inc., Lawrence, Mass.) were applied to provide the illumination for image collection. A Spectralon™ white reference panel with nearly 99% reflectance (Labsphere, North Sutton, N.H.) was employed as a reference. The camera dark image and the white reflectance image were recorded prior to the acquisition of the hyperspectral images of the cucumbers each day. During the scanning process, room lights were turned off to prevent interference from ambient light.

From each of cucumber images, three regions of interest (ROIs) were chosen from three different types of cucumber surfaces: (1) good-smooth skins (including fresh cucumbers prior to any cold storage treatments, control cucumbers that were constantly maintained at RT storage, and cucumbers that were given 0°C or 5°C cold storage treatments followed by 0 to 7 days of post-chilling RT storage); (2) good-bumpy skins (cucumbers just removed from 0°C chilling storage); and (3) chilling injured skins (cucumbers that were given 0°C or 5°C cold storage treatments followed by 0 to 7 days of post-chilling RT storage). Symptoms of chilling injury developed after cucumbers were moved into the warmer RT environment. It was observed that at the 7th day of post-chilling RT storage, cucumbers exhibited representative areas of degradation/damage caused by chilling injury, regardless of the length of time spent in cold storage at either 0°C or 5°C. Hence, chilling injured areas were determined visually from black spots visible on hyperspectral images from the 7th day of post-chilling RT storage, and then tracked back to the images collected on the 1st day of measurement (0 day post-chilling RT storage). ROI areas, varying in size from 16 to 100 pixels, were selected by using the rectangle and drawing point modes of ENVI software (Research Systems Inc., Boulder, Colo.). The mean ROI reflectance spectra were obtained for further data analysis.

PCA of ROI Spectra

To apply the PCA method, ROI spectra representing good and injured cucumber skins were first selected. Then PCA 2-class models were developed in different spectral regions, with spectral pretreatments of either multiplicative scatter correction and mean centering (MSC + MC), or multiplicative scatter correction and mean centering and also Savitzky-Golay second derivative function with 2 polynomial degree and 11 smoothing points (MSC + MC + 2nd derivative). The analysis was performed by using the PLSPlus/IQ package in Grams/32 (Version 5.2, Galactic Industrious Corp., Salem, N.H.). One-out cross-validation was used as the validation method. Classification models were established using two classes, good and injured, based on SIMCA (Soft Independent Modeling of Class Analogy) of PCA with a Mahalanobis distance and a residual spectral measurement (Galactic Industrious Corp., 1996)

Analysis of Hyperspectral Images

In-house laboratory-developed software (Kim et al., 2001) and the commercial ENVI 3.2 software package (Research Systems, Inc., Boulder, Colo.) were used for the analysis of hyperspectral images. Prior to algorithm and PCA

image analysis, images at 620 nm were processed with binary function at a threshold of 0.75% of reflectance intensity to create a mask for the cucumber surface in each image. The threshold value was determined by visual observation so as to exclude the image of background material.

Results and Discussion

Spectral Features of Good-Smooth and Injured Cucumber Skins

Figure 1 shows the representative images, at 675 nm (upper) and 756 nm (lower), of a cucumber at the stages of (a) 0-day, (b) 3-day, and (c) 7-day post chilling RT storage after an 8-day period of 0˚C cold storage treatment. Different degrees of decay and multiple sites of injury induced by the chilling treatment are clearly visible on the cucumber. Generally, damaged skins were more easily identified from the 756-nm images than from the 675-nm images. The set of images shown in figure 1 was chosen for analysis not only due to the extreme and rapid change in color appearance exhibited by the chilling damaged portions, but also due to the apparent common trends exhibited in these images that were shared among the images of other chilling injured cucumbers.

Figure 2 shows typical ROI reflectance spectra of good-smooth and injured cucumber skins in the 450- to 950-nm region, extracted from the images shown in figure 1. The progression of spectral features represents the formation of black spots on cucumber skins within 7 days of post-chilling RT storage. As the post-chilling RT storage time increased, the relative reflectance intensity was clearly observed to decrease over the entire spectral region. This reduced reflectance intensity was consistent with visual observation of damaged spots on cucumbers, i.e., the gradual appearance of dark/black color and the extinction of regular green color. The Fresh spectrum in figure 2 was from a fresh cucumber skin, which appeared bright green in color. An intense absorption near 675 nm indicates the existence of chlorophyll *a* species, a major pigment in fresh cucumber (Gross, 1991). The spectrum (f) at the bottom, from an area of severe chilling injury, showed a completely different feature to that of the Fresh spectrum. As expected, no distinctive features were to be seen in spectrum (f), primarily due to the appearance of dark color in severe chilling injured skins. The progression of spectra (a) through (e) represents the development of chilling injury from trace to slight, moderate and severe degrees of damage. Although figure 2 shows the existence of distinct spectral differences between good-smooth and chilling-damaged cucumber skins, it was still challenging to identify chilling injured portions, partly because of slight injuries on individual cucumbers and partly because of great variations in color appearance from one cucumber to another. Therefore, a number of spectral classification techniques were attempted for a large number of cucumber samples.

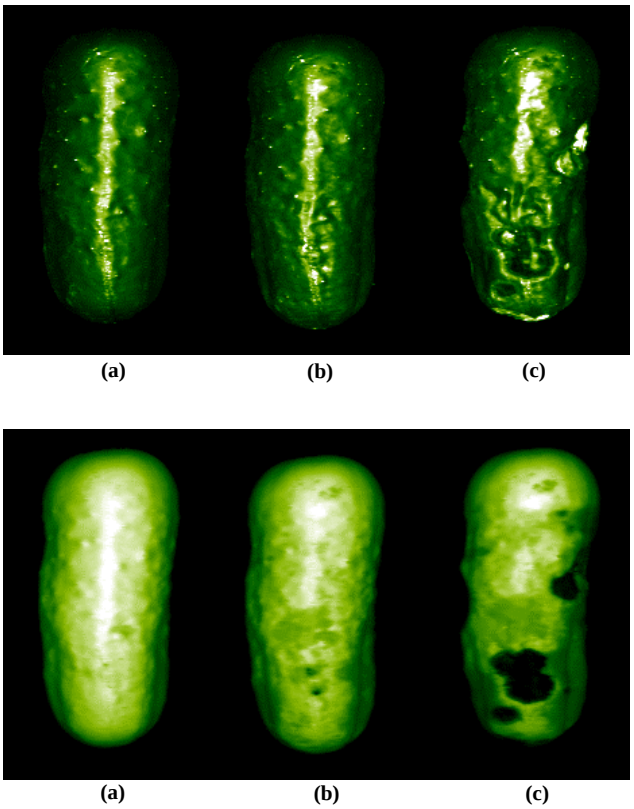

Figure 1. Hyperspectral images, at 675 nm (upper) and 756 nm (lower), of a cucumber at the stages of (a) 0-day, (b) 3-day, and (c) 7-day post chilling RT storage after an 8-day period of 0°C cold storage treatment.

Algorithms for Classifying the ROI Spectra of Good and Injured Cucumber Skins

Figure 3 shows difference spectra that were calculated by subtracting the average spectrum of the seven ROI spectra in figure 2 from each spectrum. The difference curves clearly show the large variations in the 700- to 850-nm region between good-smooth and chilling damaged skins. There are at least three negative peaks near 756, 811, and 904 nm, which fluctuate greatly. However, there is little variation for the chlorophyll *a* absorption near 670 nm. In general, the reflectance intensities at 756, 811, and 904 nm decreased in the progression from fresh skin to chilling damaged ones, and the degree of reduction depended on the length of the post-chilling RT storage period. The 756-nm band in visible region could be assigned to degraded species of chlorophylls

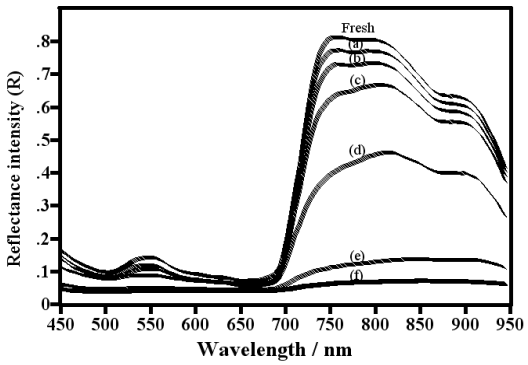

Figure 2. Representative ROI reflectance spectra of good-smooth and injured cucumber skins. They were associated with the process of turning black from bright green appearance on cucumber skins induced by chilling treatment at 0°C plus post-chilling 0-day (a), 1-day (b), 2-day (c), 3-day (d), 5-day (e), and 7-day (f) RT storage. A ROI spectrum of Fresh cucumber skin was included for comparison.

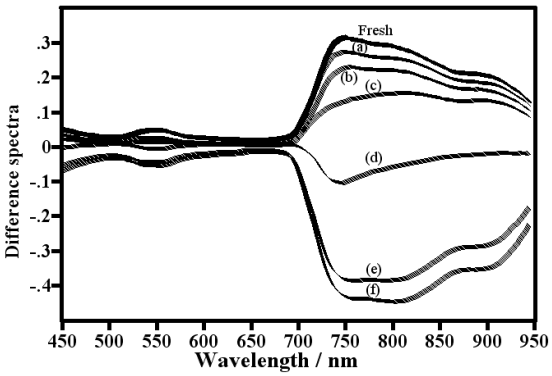

Figure 3. ROI difference spectra corresponding to the post-chilling RT storage time-dependent variations of reflectance intensities.

(Vernon and Seely, 1966), and the 811- and 904-nm bands in NIR region to N-H and C-H vibrations (Osborne et al., 1993).

Therefore, it was of interest to examine whether good-smooth and injured cucumber skins could be distinguished based on a reflectance intensity difference. We developed a number of algorithms using three bands at 756, 811, and 904 nm, with the combination of both two- (three-) band ratio/subtraction algorithms and either the use of spectral reflectance (R) or log (1/R) readings. We found that the two-band ratio ($Q_{811/756}$) given in equation 1 provided the best separation results:

$$Q_{811/756} = R_{811\ nm} / R_{756\ nm} \quad (1)$$

where $Q_{811/756}$ represents a quotient of spectral reflectances, and $R_{811\ nm}$ and $R_{756\ nm}$ are reflectances at 811 and 756 nm, respectively.

Figure 4 shows the plot of the $Q_{811/756}$ values versus post-chilling RT storage time for 22 cucumbers that were given different periods of cold storage at 0°C. Plot A (upper) shows the $Q_{811/756}$ values from areas where at least one severe black spot had developed on the cucumber by the 7th day of post-chilling RT storage; plot B (middle) shows the values from areas where at least one moderate injury spot (non black) had developed on individual cucumber at the 7th post-chilling day; and plot C (lower) shows the values from good-smooth areas that showed a consistent green appearance on the cucumber through the 7th post-chilling day. As a comparison, fresh samples prior to chilling treatments were also included in the plots, labeled as Fresh. It can be seen that in plots (A) and (B), the $Q_{811/756}$ value increased steadily and became more scattered with the increase in RT storage time, whereas $Q_{811/756}$ value stayed relatively consistent for non-damaged (good-smooth) skins (C). Due to the difference in the degree of chilling injury, it is reasonable to observe that $Q_{811/756}$ values in figure 4B generally fall between the range of those in figure 4A and C. Also, figure 4A indicates an obvious increment in $Q_{811/756}$ value after approximately 2 to 3 days post-chilling RT storage. The $Q_{811/756}$ values in both figure 4A and B suggest that degradation of chilling injured spots develops quickly after 2 to 3 days in RT storage, with the first 0 to 2 days of RT storage corresponding well to trace and slight degrees of chilling injury, and the following 3 to 7 days of RT storage to moderate and severe injury.

Analysis of the $Q_{811/756}$ values in figure 4 suggested that $Q_{811/756}$ values range from 0.95 to 1.02 for most good-smooth cucumber skins and from 1.02 to 1.30 for obviously damaged

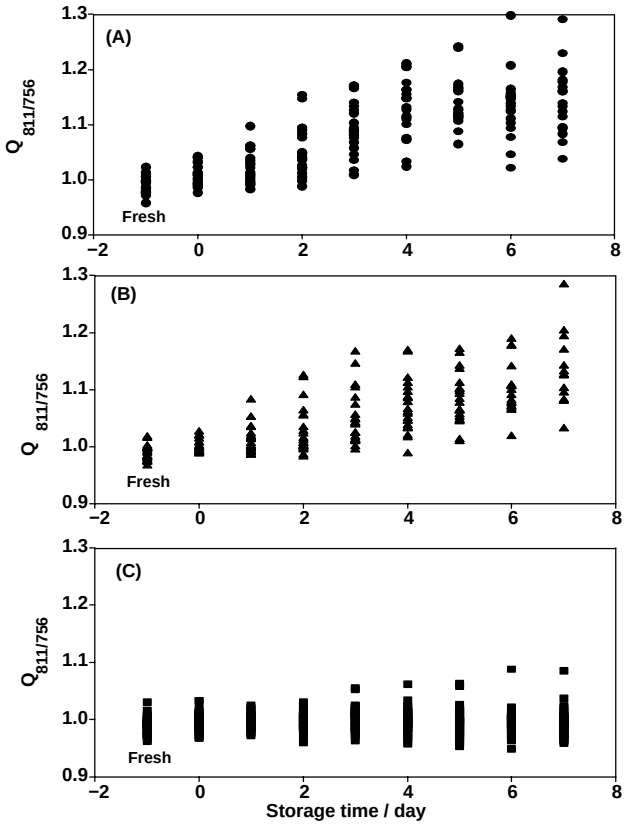

Figure 4. Plots of the $Q_{811/756}$ values versus post-chilling RT storage time for cucumbers undergone different periods of chilling treatment at 0°C; (A) appearance of at least one severe black spot at 7th day, (B) appearance of at least one moderate injury spot (non black) at 7th day, and (C) consistent appearance of good-smooth spot a 7th day. For comparison, fresh samples before the chilling treatments were also included.

cucumber skins. With a set threshold value of 1.02, (i.e., a sample was classified as good skin class when $Q_{811/756} < 1.02$ and as injured skin otherwise), 93.7% of good-smooth skin samples and 92.6 % of chilling injured spots with the 3 to 7 days RT storage were correctly classified (table 1). However, a relatively low separation rate (41.7%) for injury with the first 2 days of RT storage was observed, probably due to the following possible factors: (1) chilling damaged spots at trace and slight levels were similar to good-smooth spots in physical appearance and chemical compositions, (2) chilling injury symptoms had not started to develop for some cucumbers, and (3) chilling damaged skins had recovered to become good spots.

One of the challenges in cucumber chilling injury detection is that cucumbers with bumpy skins normally exhibit dark color and closely resemble chilling injured spots. Equation 1 algorithm was applied to good-bumpy samples, and a correct classification of 96.7% was reached (table 1). The algorithm was also applied to other cucumbers, such as cucumbers at the 0 to 7 days post-chilling RT stages following 5°C cold storage treatment, fresh cucumbers, and RT control cucumbers. The results shown in table 1 indicate positive identification of over 95% for chilling injured samples at 5°C plus the 3 to 7 days RT storage and good-smooth skins (fresh and control), 85.8% correct classification for good-smooth skins at 0 to 7 days post-chilling RT storage after 5°C cold treatment, and 63.3%

Table 1. Correct classification of two-group, good and injured cucumber skins, from ROI spectra using algorithms.[a][b]

	Calibration Set[c]			Test Set								
Algorithm	Good-Smooth at 0°C (n = 285)	Injury at 0°C and 3-7 days (n = 204)	Avg.	Injury at 0°C and 0-2 days (n = 132)	Good-Bumpy at 0°C (n = 122)	Good-Smooth at 5°C (n = 204)	Injury at 5°C and 0-2 days (n = 30)	Injury at 5°C and 3-7 days (n = 44)	Good-Smooth (Fresh) (n = 123)	Good-Smooth (Control) (n = 168)	Avg.[d]	Threshold
$Q_{811/756}$	93.7%	92.6%	93.1%	41.7%	96.7%	85.8%	63.3%	95.4%	96.8%	98.8%	82.6% (94.7%)	1.02
$S_{675/560}$	84.6%	84.3%	84.4%	49.2%	16.4%	99.5%	50.0%	81.8%	74.8%	32.1%	57.7% (60.9%)	0.30

[a] Sample sets of good-smooth at 0°C, injury at 0°C, good-smooth at 5°C, injury at 5°C, and good-smooth (control) were undergone 0 to 7 days post-chilling room temperature (RT) storage; category of good-bumpy at 0°C was without room temperature storage after the chilling treatment; group of good-smooth (fresh) was without chilling and room temperature treatments.

[b] Number in parenthesis was mean of correct classification for test sets without the consideration of Injury at 0°C and 5°C with post-chilling 0 to 2 days RT storage.

[c] Due to insignificant injury symptoms, samples at 0 to 2 days post-chilling RT storage after 0°C cold storage treatment were excluded from the calibration set.

[d] Numbers in parenthesis excluded the 0 to 2 days RT storage data.

correct discrimination for injury samples from cucumbers at 0 to 2 days RT storage after 5°C cold storage treatment. The overall correct classification in the calibration and test sets were 93.1% and 82.6%, respectively. The separation rate in the test set improved to 94.7% from 82.6% when the skins from cucumbers at 0 to 2 days RT storage after (0°C and 5°C) cold storage treatments were excluded.

To address the color effect from chlorophylls (675 nm) and carotenoids (560 nm), we also tested a variety of algorithms using the 560- and 675-nm spectral reflectances or log (1/R) readings, and obtained the best separation by the following equation (Liu et al., 2005):

$$S_{675/560} = \log (1/R_{675\ nm}) - \log (1/R_{560\ nm}) \qquad (2)$$

where $S_{675/560}$ represents the difference in log (1/R) of spectral reflectances, and $R_{675\ nm}$ and $R_{560\ nm}$ are reflectances at 675 and 560 nm, respectively

Figure 5 plots the $S_{675/560}$ values for the same data set as shown in figure 4. Although there was a scattered distribution for the $S_{675/560}$ values, the specific tendency of decreasing $S_{675/560}$ value for chilling injured skins (A) and (B) was evident, so did the relatively constant $S_{675/560}$ value for good-smooth skins (C). A relative difference in $S_{675/560}$ value existed between good-smooth skins and injured ones, and the obvious decrease in $S_{675/560}$ value occurs around 2 to 3 days of post-chilling RT storage (A), which is consistent with the result obtained by equation 1.

Statistics on $S_{675/560}$ (table 1) indicated that, with a threshold of 0.30 (i.e., a sample was classified as good skin class when $S_{675/560} > 0.30$ and as injured otherwise), $S_{675/560}$ value only improves the separation of two types of samples, injury at 0 to 2 days post-chilling RT storage after 0°C cold storage treatment, and good-smooth skins at 0 to 7 days post-chilling RT storage after 5°C cold storage. However, the correct identification of good-bumpy skins at 0°C and good-smooth skins (control) in the test set reached only 16.4% and 32.1%, respectively; both are much lower than the classification rates from the $Q_{811/756}$ algorithm, indicating that the chlorophyll band alone is not sensitive enough to reflect the subtle physical and chemical variations among chilling damaged skins (there are minimum variations at both 560 and 675 nm in fig. 3).

In summary, the $Q_{811/756}$ algorithm provided better identification than the $S_{675/560}$ method, with a classification accuracy of 93.1% for the calibration set and 82.6% for the test set. It performed more accurately than the $S_{675/560}$ algorithm for seven of nine subsets, and yielded the medium and acceptable separation for the remaining two sample sets. The result demonstrated the importance of the dual bands, 811 and 756 nm, in the detection of chilling injured areas in cucumbers. This observation is in good agreement with hyperspectral imaging detection of bruises, defects, and feces on apples (Lu et al., 1999; Mehl et al., 2004), in which both the 700- to 900-nm visible/NIR region and three visible/NIR bands (685, 722, and 869 nm) were found to be

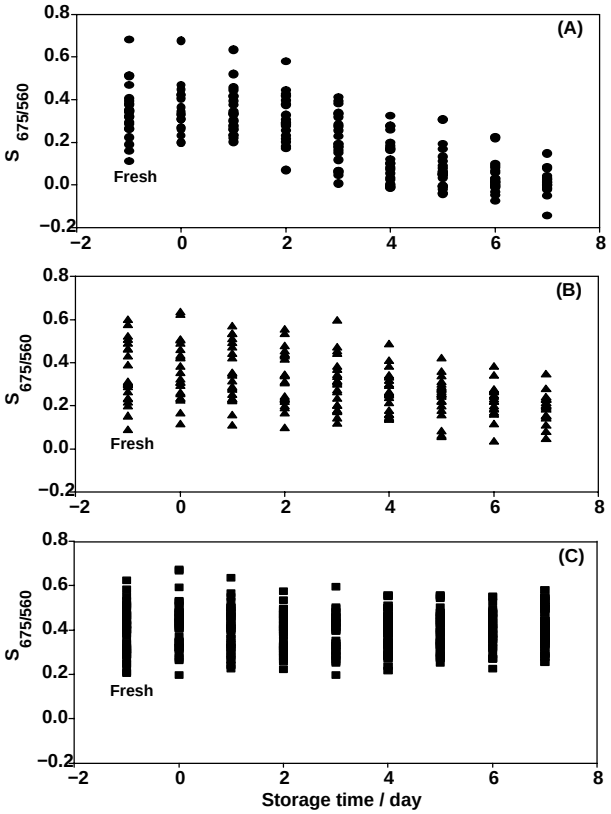

Figure 5. Plots of the $S_{675/560}$ values versus post-chilling RT storage time for cucumbers that have undergone different periods of chilling treatment at 0°C; (A) appearance of at least one severe black spot at 7th day, (B) appearance of at least one moderate injury spot (non black) at 7th day, and (C) consistent appearance of good-smooth spot a 7th day. For comparison, fresh samples before the chilling treatments were also included.

efficient in revealing imaging differences between normal and abnormal apple skins.

PCA Classification Model for ROI Spectra of Good and Injured Skin Classes

The usefulness of both the 811- and 756-nm bands in detecting the chilling damages on cucumber skins was observed from the successful classification results of using $Q_{811/756}$ algorithm. To validate the findings, multivariate data analysis using the PCA approach was attempted. Because of insignificant injury symptoms for samples at 0 to 2 days post-chilling RT storage after 0°C cold storage treatment, the spectral data of these samples were excluded from the calibration set. Therefore, a total of 489 ROI spectra, representing 285 good-smooth skins at 0 to 7 days post-chilling RT storage after 0°C cold storage treatment and 204 injured skins at 3 to 7 days post-chilling RT storage after 0°C cold storage treatment, were loaded into the PLSplus/IQ package in Grams/32 for discriminant analysis. The calibration set consisted of 190 good-smooth and 136 injury spectra; the remaining 163 spectra (95 good-smooth, 68 injury), selected by every third sample in the total data set, were used for model validation. A classification model was first developed in 450- to 950-nm region using two classes (good and injured) and with MSC + MC spectral pretreatment. For each of the two classes, the optimal number of factors was suggested to be 11. By applying two SIMCA classes (good and injured) to all 489 spectra in the calibration and validation sets and employing the class assignment rule of lower Mahalanobis distance, the sample was identified as either good skin or injured skin. The results showed that it was possible to distinguish good-smooth skins from injured ones with a correct classification of 91.9% (table 2).

An independent test set, consisting of 823 cucumber skins under a variety of conditions, was used to examine the performance of the 2-class model on the basis of good and injured skins. When the model was applied to the test set, good-smooth spots from fresh and control cucumbers as well as chilling injured spots at 3 to 7 days RT storage after 5°C cold storage treatment were easily identified with a success rate of over 98%. However, at least 40% of injured skins at 0 to 2 days RT storage after either 0°C or 5°C cold storage treatment were misclassified as good-smooth skins (table 2). Overall, the correct classification rate for the test set was 93.1% when the samples from injured spots at 0 to 2 days RT storage were excluded.

As a comparison, the discriminant model for the same data set was developed in the narrow spectral region of 733 to 848 nm, and the results are also summarized in table 2. It is encouraging to observe a slight increase in classification accuracy for the calibration set, from 91.9% to 92.3%. There was also excellent performance for samples in test set, including good-bumpy skins at 0°C, good-smooth skins at 5°C, injured spots at 3 to 7 days RT storage after 5°C, and good-smooth spots from fresh and control cucumbers. Notably, the correct prediction of good-bumpy skins at 0°C and good-smooth skins at 5°C was greatly improved. However, the correct prediction of injured spots (0°C and 5°C) at 0 to 2 days RT storage was reduced. The classification accuracy for the test set was as high as 98.4% when omitting the consideration of samples from injured spots (0°C and 5°C) at 0 to 2 days RT storage.

PCA models on the reflectance data with MSC + MC +2nd derivative pretreatment resulted in a decreased classification rate, not only for the calibration set but also for the test set (table 2). However, the results showed that chilling injured spots at 0 to 2 days post-chilling RT storage (after either 0°C or 5°C cold storage) were more easily identified using the second derivative spectral pretreatment than using raw reflectance data, but at the significant expense of the other sample types. Therefore, as a compromise, the model using raw reflectance spectra in the 733- to 848-nm region was determined to provide the best classification results among the models tested.

Comparison of the results shown in tables 1 and 2 suggests that classification using the simple dual-band ratio algorithm and using multivariate data analysis are comparable and consistent. Generally, the $Q_{811/756}$ algorithm yielded a slightly better discrimination rate than the PCA model for injured skins at 0 to 2 days RT storage. The results also indicated the importance of spectral bands covering the region of 733 and 848 nm in the detection of chilling injury on cucumber surface. Obviously, the $Q_{811/756}$ algorithm approach is preferable for the following reasons: (1) it is simple and there is no need for a calibration model; (2) it reduces the influence of chlorophyll and carotenoid components; and (3) it could be useful for the implementation of a

Table 2. Correct classification of two-group, good and injured cucumber skins, from ROI spectra using 2-class PCA model[a][b]

	Calibration Set[c]			Test Set							
Spectral Mode/ Region	Calibration (n = 326)	Validation (n = 163)	Avg.	Injury at 0°C and 0-2 days (n = 132)	Good-Bumpy at 0°C (n = 122)	Good-Smooth at 5°C (n = 204)	Injury at 5°C and 0-2 days (n = 30)	Injury at 5°C and 3-7 days (n = 44)	Good-Smooth (Fresh) (n = 123)	Good-Smooth (Control) (n = 168)	Avg.[d]
Raw/ 450-950 nm	93.6%	90.2%	91.9%	38.6%	77.9%	89.2%	60.0%	100%	98.4%	100%	80.5% (93.1%)
Raw/ 733-848 nm	94.5%	90.2%	92.3%	24.2%	99.2%	99.5%	43.3%	93.2%	100%	100%	79.9% (98.4%)
2nd derivative/ 450-950 nm	86.2%	83.4%	84.8%	59.8%	81.2%	60.3%	70.0%	100%	87.0%	98.8%	79.6% (85.4%)
2nd derivative/ 450-950 nm	84.4%	86.5%	85.4%	51.5%	63.1%	63.7%	80.0%	93.7%	85.4%	77.4%	73.5% (76.7%)

[a] Spectral pretreatment with mean centering (MC) + multiplicative scatter correction (MSC).
[b] Refer to table 1 for the description of sample subgroups in test set.
[c] Calibration set consisted of 190 good and 136 injury spectra, and validation set included 95 good and 68 injury spectra (see text).
[d] Numbers in parenthesis excluded the 0 to 2 days RT storage data.

dual-band multispectral imaging system for on-line/off-line inspection of cucumber injuries and defects.

Feasibilty of Detecting Chilling Injury At Early RT Storage

The above results demonstrated successful discrimination between good skins and injured skins at 3 to 7 days post-chilling RT storage, but also revealed the difficulty of positive identification of chilling injury at 0 to 2 days post-chilling RT storage. Here, we examined the chilling damaged samples at 0 to 4 days post-chilling RT storage (after 0°C cold storage) by subgrouping them into two groups, one representing the appearance of at least one severe black spot on individual cucumber skin at 7th day (A) and another the appearance of at least one moderate injury spot (non black) on individual cucumber at 7th day (B). As shown in table 3, the classification rates of both A and B samples steadily increased as expected with increasing RT storage time, and A samples were slightly easier to be identified than B samples. At least table 3 suggests the possibility of detecting the chilling injury at early RT storage, especially at the initial 0 to 2 days RT storage. It is suspected that detection results would be improved if the samples without obvious symptoms of chilling injury were separated from the data set.

Comparison of Dual-Band Algorithm and PCA Models for Detection of Chilling Injury

The above results demonstrated the effectiveness of the dual-band ratio algorithm for the classification of ROI spectra of good and injured cucumber skins. Hence, it was of great interest to apply such a ratio algorithm in the analysis of hyperspectral images. Figure 6a shows the resulted dual-band ratio ($Q_{811/756}$) images of a cucumber undergone the 8-day chilling treatment at 0°C plus post-chilling 0-, 2-, 4-, and 6-day RT storage. The existence of at least three types of cucumber skins, good (shown in white), moderate chilling damaged/non-black (shown in slightly dark), and severe chilling damaged/black (shown in heavily dark), was clearly indicated. With the RT storage, the obvious appearance and increase in number of dark areas suggested considerable occurrence of chilling injury. Also, the variations in relative darkness implied the different levels of chilling damages, which in turn, reflected the sequential order in the development of chilling injury symptoms. Hence, it is possible to assign white areas as normal skins, and dark areas as injured ones. In fact, the ratio values for good and injured skins were in consistent agreement with those from earlier ROI data, making a possible threshold setting for the classification of chilling injured skins. In addition, no dark spots were observed in Fresh cucumber, and few injured areas were distinguishable in the cucumber immediately after the chilling treatment (0-day), as expected.

Although figure 6a showed an obvious discrimination between good and injured spots, these results could not be used alone to evaluate the performance of the dual-band algorithm in the detection of chilling injury quantitatively, because the exact number of chilling injured spots could not be easily determined. However, two possible methods of validating the effectiveness of the dual-band algorithm were to process the same images by using different algorithms/ multivariate data approach, and to analyze the known images (whose conditions were clear) by using the same algorithm.

To confirm the results observed from the dual-band algorithm, PCA was applied to extract useful information from the images in full or narrow spectral regions. Careful examination of a number of principal component (PC) images revealed that there was no large difference in the detection of chilling injured spots between the full spectral region (450 to 950 nm) and the narrow region (733 to 848 nm), which was in good agreement with the

(a) $Q_{811/756}$

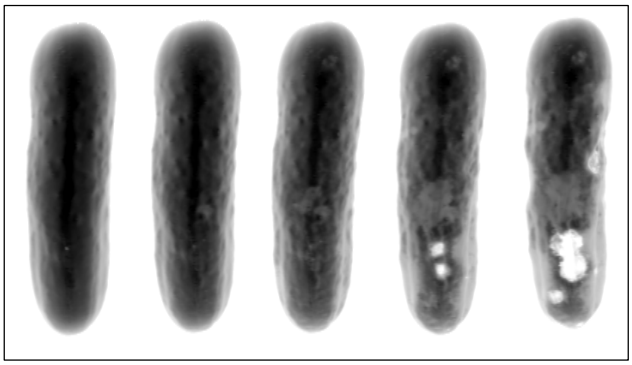

(b) PCA

Figure 6. Comparison of processed images from dual-band ratio (a) and the first PC band (b). The images, from left to right in either (a) or (b), show the cucumber before the 8-day chilling treatment at 0°C and after the treatment at the stages of 0-, 2-, 4-, and 6-day post-chilling RT storage, respectively.

Table 3. Percentage (%) of correct identification of chilling injury on cucumbers at 0°C with the 0- to 4 days post-chilling RT storage from ROIs of hyperspectral imaging.[a]

	0 Day		1st Day		2nd Day		3rd Day		4th Day	
Algorithm/Models	A[b]	B[c]	A	B	A	B	A	B	A	B
$Q_{811/756}$	40.9	22.7	45.4	27.2	72.7	40.9	90.9	68.2	100	86.4
Raw/733-848 nm	13.6	0	27.2	18.2	59.1	27.2	86.4	50.0	95.4	81.8

[a] Number of samples was 22 for individual A (severe injury) and B (moderate injury) groups.
[b] Appearance of at least one severe black spot on individual cucumber skin at 7th day (severe injury).
[c] Appearance of at least one moderate injury spot (non black/white) on individual cucumber at 7th day (moderate injury).

classification of ROI spectral data. Figure 6b shows the score of the cucumber image with respect to the first PC from the narrow region for the same cucumbers as those shown in figure 6a. As the first PC band explains more than 99% of the total variance, it contains the largest amounts of data variance. The remaining PC bands represent other details that are not common to all cucumbers, and some specific information might be lost in these PCs. In figure 6b, the first PC can be seen to enhance the contrast between the good skins (darkest areas), moderately injured spots (gray areas), and severely injured spots (white areas), although some difficulty may remain in locating some of the moderately injured spots.

Generally, the dual-band ratio algorithm produced images were nearly as effective in identifying chilling injury as those produced using the PCA method. Of particular interest, bumpy skins were correctly identified in dual-band ratio images (fig. 6a), whereas they were easily misclassified in the PC images (fig. 6b). The results suggested that the dual-band ratio analysis neither fails to detect the chilling injured spots nor overreact to non-chilling fractions. Consequently, the dual-band ratio algorithm is reliable and could be used to design a multispectral imaging system for chilling injury detection.

Test of Dual-Band Algorithm in the Detection of Chilling Injury

Hyperspectral images of cucumbers with different treatments were collected to test the previous algorithm. Figure 7 shows the results for a cucumber before 12-day cold storage treatment at 5°C (Fresh) and then following the cold treatment plus 0-, 2-, 4-, and 6-day of post-chilling RT storage. For comparison, figure 8 depicts the results for a control sample cucumber (given no chilling treatment) at 4-day intervals during RT storage. Chilling damaged spots (shown as dark areas in fig. 7a) started to appear for the treated cucumber at 2-day RT storage and subsequently became more extensive with additional RT storage time. As expected, no obvious chilling injury was observed in the cucumbers at the Fresh and 0-day RT storage stages. The second PC nearly matched the dual-band ratio algorithm in positively identifying chilling-injured spots (the darkest areas in fig. 7b). However, PCA method also misclassified bumpy skins as chilling damaged ones, as can be seen by the darker spots in figure 7b for the Fresh and 0-day RT cucumbers.

Obviously, control samples, those always stored at RT, should not have any chilling injury symptoms. Hence, it is reasonable to observe such unaffected cucumber surfaces, besides the native spots (fig. 8). Similarly, the third PC images showed more recognizable bumpy skins than dual-band ratio images.

Comparison of the images in figures 6 through 8 suggested that the correct detection of chilling injured areas from simple dual-band ratio algorithm is well validated by both additional processing method and the cucumbers at different conditions. Therefore, the analysis from the dual-band ratio algorithm is consistent, reliable, and effective. Major advantages of utilizing the 811- and 756-nm bands are to reduce the influence from the chlorophyll component and to eliminate the likelihood of misclassifying bumpy skins as injured ones.

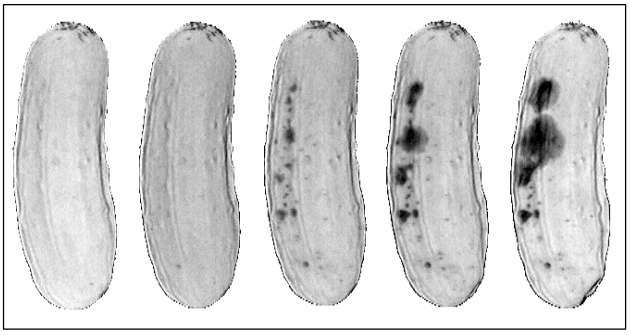

(a) $Q_{811/756}$

(b) PCA

Figure 7. Comparison of processed images from dual-band ratio (a) and the second PC band (b). The images, from left to right in either (a) or (b), show the cucumber before the 12-day chilling treatment at 5°C and after the treatment at the stages of 0-, 2-, 4-, and 6-day post-chilling RT storage, respectively.

(a) $Q_{811/756}$

(b) PCA

Figure 8. Comparison of processed images from dual-band ratio (a) and the third PC band (b). The images, from left to right in either (a) or (b), show a control sample cucumber at the stages of Fresh, 4-, 8-, 12-, and 16-day RT storage, respectively.

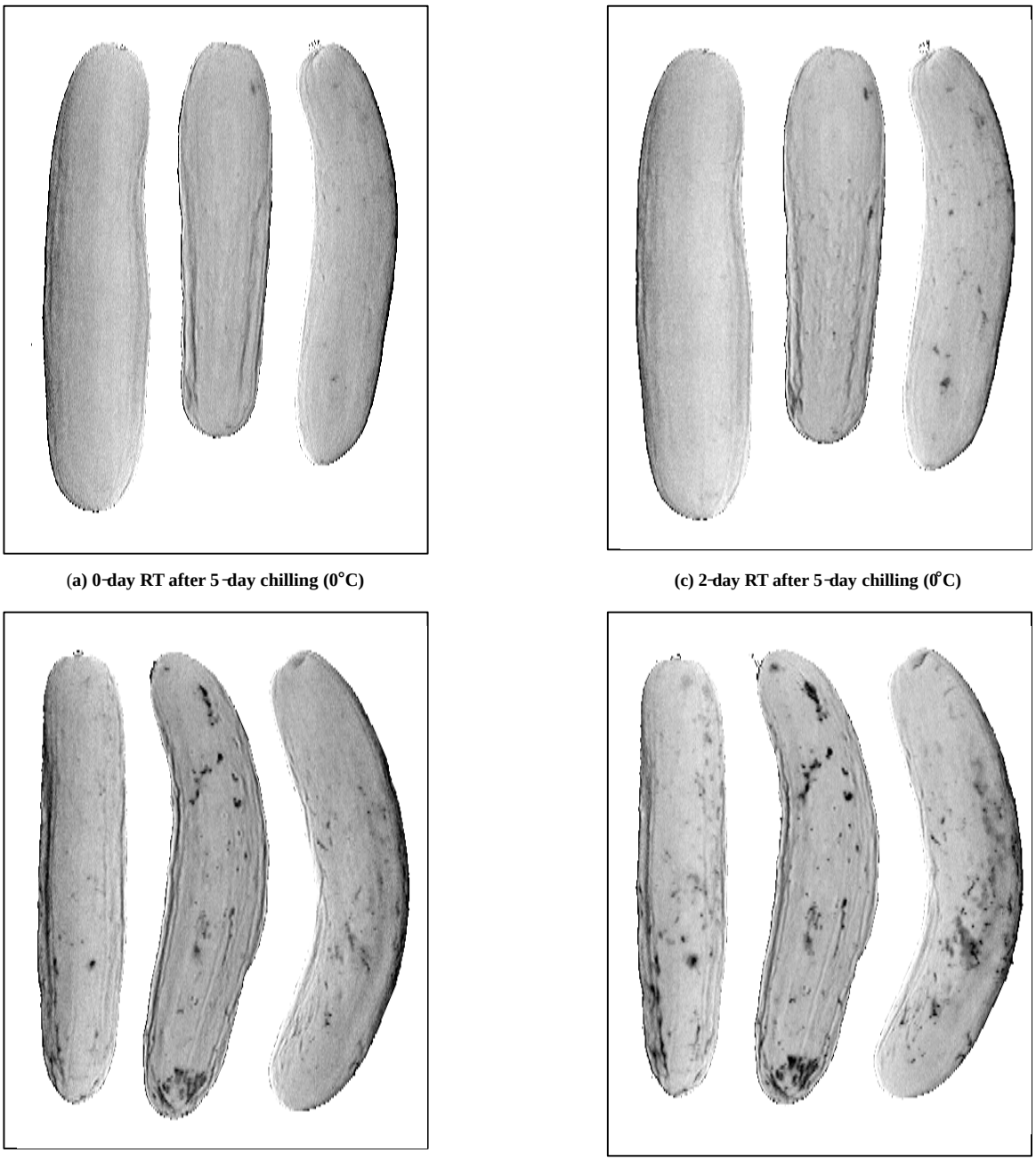

(a) 0-day RT after 5-day chilling (0°C)

(c) 2-day RT after 5-day chilling (0°C)

(b) 0-day RT after 14-day chilling (0°C)

(d) 2-day RT after 14-day chilling (0°C)

Figure 9. Dual-band images of cucumbers that were given 5- and 14-day chilling treatments at 0°C, at the stages of 0- and 2-day post-chilling RT storage. (a) 0-day RT after 5-day chilling, (b) 0-day RT after 14-day chilling, (c) 2-day RT after 5-day chilling, and (d) 2-day RT after 14-day chilling.

Detection of Early Stage Chilling Injury Using Dual-Band Algorithm

The obtained results suggested that the dual-band algorithm might be successfully implemented in image analysis for the detection of chilling injury in cucumbers. However, it revealed the difficulty of singling out the chilling injured portions in cucumbers that were scanned immediately after the chilling treatments. To understand the effect of both chilling temperature (0°C vs. 5°C) and the subsequent RT storage on cucumbers, figure 9a through 9d show dual-band images of two sets of cucumbers given either 5 or 14 days of 0°C cold storage, and figure 10a through 10d show dual-band images of two sets of cucumbers given either 5 or 14 days of 5°C. Each set of cucumbers can be compared at the stages of 0- and 2-day post-chilling RT storage. As anticipated, there were more chilling injured areas in cucumbers with longer chilling treatment (fig. 9a vs. 9b; fig. 10a vs. 10b), and with lower chilling temperature (fig. 9 vs. fig. 10). After the first 2-day of RT storage, symptoms of chilling damages developed obviously and extensively (fig. 9c, 9d, 10c, and 10d), making chilling injured spots more easily identified. Hence, detection of chilling injury in cucumbers strongly depended on the duration and temperature of chilling treatment, and also on the period of post-chilling storage.

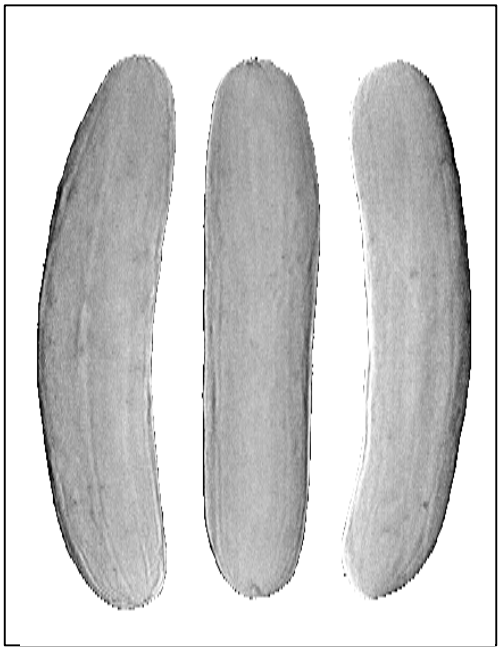

(a) 0-day RT after 5-day chilling (5°C)

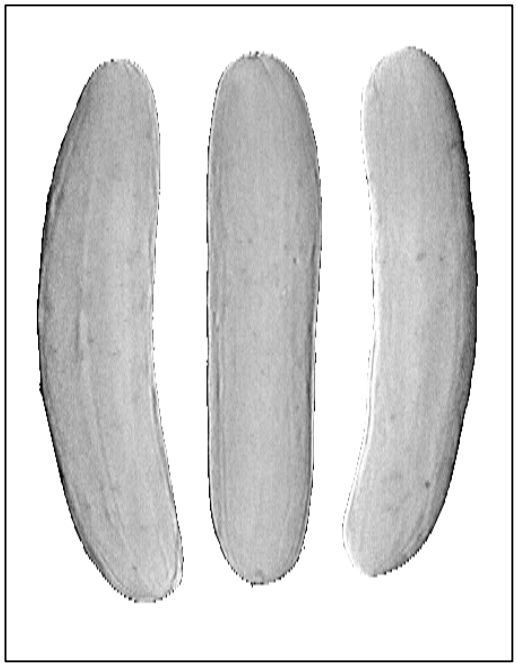

(c) 2-day RT after 5-day chilling (5 °C)

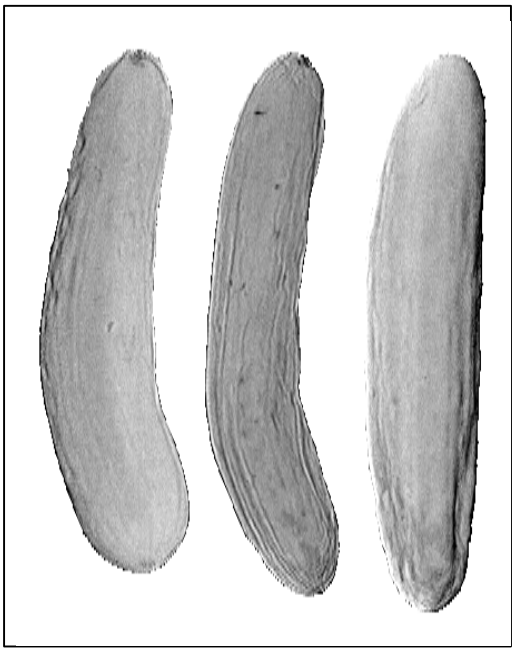

(b) 0-day RT after 14-day chilling (5°C)

(d) 2-day RT after 14-day chilling (5 °C)

Figure 10. Dual-band images of cucumbers that were given 5- and 14-day chilling treatments at 5°C, at the stages of 0- and 2-day RT storage. (a) 0-day RT after 5-day chilling, (b) 0-day RT after 14-day chilling, (c) 2-day RT after 5-day chilling, and (d) 2-day RT after 14-day chilling.

CONCLUSIONS

The results of this study demonstrate the effectiveness of hyperspectral imaging technique in the characterization of the changes associated with chilling injury of whole cucumbers. Spectral features of chilling damaged skins varied from higher reflectance to lower reflectance with increasing time at post-chilling room temperature (RT) storage. Such a spectral difference forms the basis for the identification of injured skins in cucumbers.

A number of methodologies were applied to analyze and classify ROI spectra of good and chilling injured cucumber skins. The results revealed that both a dual-band algorithm and a multivariate PCA model could be used to perform the classification analysis between good and injured skins classes with a great success of over 90%. Particularly, the findings of the $Q_{811/756}$ algorithm and a narrow 733- to 848-nm spectral region are the most important in the development of a multispectral imaging system for on-line

inspection of cucumber injuries and defects. This spectral region can reduce the effect of the natural pigments, such as chlorophylls and carotenoids, on the separation of good-bumpy skins from chilling damaged ones.

Application of the dual-band ratio algorithm to the analysis of hyperspectral images for the detection of chilling injury was well confirmed by additional processing method and cucumbers at various conditions. Dual-band images showed more correct separations than PC images. Consequently, the $Q_{811/756}$ algorithm can be incorporated into a dual-band multispectral imaging system.

Notably, detection of chilling injury at early stage with insignificant injury symptom was relatively difficult, because the development of chilling injury was affected by the elapsed time after chilling damage, and also the period and temperature of chilling environment.

ACKNOWLEDGEMENT

The authors wish to express their sincere thanks to Ms. Xuemei Cheng, University of Maryland, for assisting in the collection of Hyperspectral images of cucumbers at the USDA Instrumentation and Sensing Laboratory.

REFERENCES

Galactic Industrious Corp. 1996. *PLSplus/IQ for GRAMS/32 and GRAMS/386*. Galactic Industrious Corp., Salem, N.H.

Gross, J. 1991. *Pigments in Vegetables.* New York: Van Nostrand Reinhold.

Kim, M. S., Y. R. Chen, and P. M. Mehl. 2001. Hyperspectral reflectance and fluorescence imaging system for food quality and safety. *Transaction of the ASAE* 44(3): 721-729.

Kim, M. S., A. M. Lefcourt, K. Chao, Y. R. Chen, I. Kim, and D. E. Chan. 2002. Multispectral detection of fecal contamination on apples based on hyperspectral imagery: Part I. Application of visible and near-infrared reflectance imaging. *Transaction of the ASAE* 45(6): 2027-2037.

Lawrence, K. C., W. R. Windham, B. Park, and R. J. Buhr. 2001. Hyperspectral imaging system for identification of fecal and ingesta contamination on poultry carcasses. ASAE Paper No. 013076. St. Joseph, Mich.: ASAE.

Liu, Y., W. R. Windham, K. C. Lawrence, and B. Park. 2003. Simple algorithms for the classification of visible/near-infrared and hyperspectral imaging spectra of chicken skins, feces, and fecal contaminated skins. *Applied Spectroscopy* 57(12): 1609-1612.

Liu, Y., Y.- R. Chen, C. Y. Wang, D. E. Chan, and M. S. Kim. 2005. Development of a simple algorithm for the detection of chilling injury in cucumbers from visible/near-infrared hyperspectral imaging. *Applied Spectroscopy* 59(1): 78-85.

Lu, R. 2003. Detection of bruises on apples using near-infrared hyperspectral imaging. *Transactions of the ASAE* 46(2): 523-530.

Lu, R., and Y. R. Chen. 1998. Hyperspectral imaging for safety inspection of food and agricultural products. *Proceedings of SPIE: Pathogen Detection and Remediation for Safe Eating* 3544: 121-133.

Lu, R., Y. R. Chen, B. Park, and K.-H. Choi. 1999. Hyperspectral imaging for detecting bruises in apples. ASAE Paper No. 993120. St. Joseph, Mich.: ASAE.

Mehl, P. M., K. Chao, M. S. Kim, and Y. R. Chan. 2002. Detection of defects on selected apple cultivars using hyperspectral and multispectral image analysis. *Applied Engineering in Agriculture* 18(2): 219-226.

Mehl, P. M., Y. R. Chen, M. S. Kim, and D. E. Chan. 2004. Development of hyperspectral imaging technique for the detection of apple surface defects and contaminations. *J. Food Engineering* 61: 67-81.

Osborne, B. G., T. Fearn, and P. H. Hindle. 1993. *Practical Near-Infrared Spectroscopy with Application in Food and Beverage Analysis,* 2nd ed. Harlow, UK: Longman Scientific & Technical.

Vernon, L. P., and G. R. Seely. 1966. *The Chlorophylls.* New York: Academic Press.

Wang, C. Y. 1993. Approaches to reduce chilling injury of fruits and vegetables. *Horticultural Reviews* 15: 63-95.

Windham, W. R., K. C. Lawrence, B. Park, and R. J. Buhr. 2003. Visible/NIR spectroscopy for characterizing fecal contamination of chicken carcasses. *Transaction of the ASAE* 46(3): 747-751.